Later Wet Seasons with More Intense Rainfall over Africa under Future Climate Change

CAROLINE M. DUNNING AND EMILY BLACK

Department of Meteorology, and National Centre for Atmospheric Science–Climate, University of Reading, Reading, United Kingdom

RICHARD P. ALLAN

Department of Meteorology, University of Reading, and National Centre for Earth Observation, Reading, United Kingdom

(Manuscript received 23 February 2018, in final form 19 September 2018)

ABSTRACT

Changes in the seasonality of precipitation over Africa have high potential for detrimental socioeconomic impacts due to high societal dependence upon seasonal rainfall. Here, for the first time we conduct a continental-scale analysis of changes in wet season characteristics under the RCP4.5 and RCP8.5 climate projection scenarios across an ensemble of CMIP5 models using an objective methodology to determine the onset and cessation of the wet season. A delay in the wet season over West Africa and the Sahel of over 5–10 days on average, and later onset of the wet season over southern Africa, is identified and associated with increasing strength of the Saharan heat low in late boreal summer and a northward shift in the position of the tropical rain belt over August–December. Over the Horn of Africa rainfall during the "short rains" season is projected to increase by over 100 mm on average by the end of the twenty-first century under the RCP8.5 scenario. Average rainfall per rainy day is projected to increase, while the number of rainy days in the wet season declines in regions of stable or declining rainfall (western and southern Africa) and remains constant in central Africa, where rainfall is projected to increase. Adaptation strategies should account for shorter wet seasons, increasing rainfall intensity, and decreasing rainfall frequency, which will have implications for crop yields and surface water supplies.

1. Introduction

Africa is acutely vulnerable to the effects of climate change. The large proportion of the population dependent upon rain-fed agriculture for their source of income and subsistence means that future changes in rainfall over Africa have high potential for detrimental socioeconomic consequences. In particular, the timing of the seasonal cycle determines the length of the growing season and agricultural yields (Vizy et al. 2015) and affects the transmission period of a number of vector-borne diseases (Tanser et al. 2003). Understanding future changes in the seasonal cycle of precipitation over Africa is crucial for establishing appropriate adaptation strategies. To assess and interpret future projections of rainfall, we require an improved understanding of the drivers and physical mechanisms behind future changes in seasonality. For the most part, coupled climate models have been found to accurately represent the seasonal cycle of precipitation over Africa (Dunning et al. 2017), affording the opportunity to investigate future projections and the associated driving mechanisms.

The combination of increased atmospheric water vapor in a warming climate (Held and Soden 2006; Allan et al. 2010; Chou et al. 2013) with changes in atmospheric circulation leads to a complex pattern of change in rainfall over the tropics, with changes in seasonality accompanying changes in rainfall amount.

Denotes content that is immediately available upon publication as open access.

Supplemental information related to this paper is available at the Journals Online website: https://doi.org/10.1175/JCLI-D-18-0102.s1.

Corresponding author: Caroline M. Dunning, c.m.dunning@reading.ac.uk

DOI: 10.1175/JCLI-D-18-0102.1

Studies documenting recent enhancements in the seasonal cycle of precipitation, with wet seasons getting wetter and dry seasons getting drier (Chou et al. 2013) and a widening of the tropical belt (Seidel et al. 2008) altering the seasonal progression of the tropical rain belt (Birner et al. 2014), imply changing rainfall seasonality in the tropics (Feng et al. 2013), which will continue under future climate change (Marvel et al. 2017).

Previous studies have examined the changes in annual or seasonal rainfall totals over Africa (Hulme et al. 2001; Lee and Wang 2014; Tierney et al. 2015; Lazenby et al. 2018). Collins et al. (2013) found increases in rainfall across central equatorial Africa in boreal winter [December–February (DJF)], particularly over East Africa, with decreases over northeast Africa and southern Africa for the end of the twenty-first century (2081–2100). In March–May (MAM) Collins et al. (2013) again show increases in rainfall over central Africa and decreases over northern and southern Africa. Patterns of change are similar in June–August (JJA) and September–November (SON) with increases over northern and northwestern Africa and decreasing rainfall over southern Africa (Collins et al. 2013).

However, the societally important rainfall, that which impacts agricultural yields and affects the transmission of vector-borne diseases, occurs during the wet season, which may not coincide with fixed meteorological seasons (Cook and Vizy 2012). For example, over the Horn of Africa the second wet season (short rains) occurs in October–December (Camberlin et al. 2009; Shongwe et al. 2011; Yang et al. 2015a). In addition, climate model simulations may contain timing biases, such as over East Africa where the first wet season (long rains; MAM) is late in coupled model simulations (Dunning et al. 2017). Furthermore, other metrics are of high importance to agriculturists in addition to the total amount of seasonal rainfall. The timing of the wet season, particularly the onset, determines planting dates and thus has large impacts upon agricultural yields (Kniveton et al. 2009).

Some studies have postulated changes in onset and cessation of the wet season by analyzing changes in rainfall amounts in the transition seasons or the months at the beginning and end of the wet season (Biasutti and Sobel 2009; Seth et al. 2013; Sylla et al. 2015); for example, Shongwe et al. (2009) identified a decline in austral spring (SON) rainfall over southern Africa and associated this with a delay in wet season onset, and Biasutti (2013) found declining rainfall in the onset months (June–July) and increasing rainfall in the demise months (September–October), implying a delay in the rainy season over West Africa. However, these studies offer no quantitative assessment of how the seasonal timing is changing and do not take into account model timing biases. Furthermore, Monerie et al. (2016) found that the delay in cessation of the West African monsoon was not correlated with the mean late monsoon precipitation change, although we would expect changing onset and cessation dates to be related to changing rainfall at the beginning and end of the wet season. Studies looking at the changing nature of seasonal timing by quantitatively calculating onset and cessation dates tend to focus on the national to regional scale (Vizy et al. 2015) or average the results over large spatial areas, such as in Christensen et al. (2013) where future projections of onset date, retreat date, and duration are averaged over a northern African and a southern African region, masking spatial variability. Marvel et al. (2017) examined changes in the seasonal cycle of zonal mean precipitation and found a later onset at tropical latitudes; however, zonal averaging masks spatial variability, especially as the progression of rainfall is not always zonally contiguous (Liebmann et al. 2012; Dunning et al. 2016).

Cook and Vizy (2012) analyzed future projections of the growing season in Africa in a single regional climate model, run with six ensemble members, with the boundary conditions determined using output from nine climate model simulations from the generation of models from phase 3 of the Coupled Model Intercomparison Project (CMIP3). The number of growing season days is calculated by comparing precipitation to potential evapotranspiration, with start and end dates computed over select regions. They find a longer growing season in the central and eastern Sahel, and reductions in length of the growing season over southern Africa and parts of the western Sahel. The increased resolution of the ensemble in phase 5 of the Coupled Model Intercomparison Project (CMIP5) enables analysis, previously only possible in regional models, to be carried out in global models. There is thus an opportunity to advance Cook and Vizy's (2012) results by examining changes across a number of global climate models from the CMIP5 generation of models, enabling the robustness of changes to be examined, using a methodology applicable across an ensemble of climate models, regardless of differences in their basic state. Furthermore, we further their discussion on the mechanisms behind future changes in seasonality.

We use an objective method for identifying the onset and cessation of the wet season and for the first time investigate changes in characteristics of African wet seasons under climate change across a large ensemble of CMIP5 models at a continental scale. Decomposing the annual cycle into a measure of seasonal timing and rainfall amount enables us to quantify changes in both

these aspects of seasonality, for regions with both one and two wet seasons per year. In addition, changes in measures of rainfall intensity are also considered. This analysis is conducted across continental Africa, enabling us to relate changes in seasonal timing with changes in the meteorological systems that drive the seasonal cycle of rainfall over Africa.

2. Methods and data

a. Model output and observational data

Daily precipitation data from 29 models used in CMIP5 (Taylor et al. 2012) were used to compute onset and cessation dates over a recent period (1980–99), a mid-twenty-first-century period (2030–49), and a period at the end of the twenty-first century (2080–99). The CMIP5 simulations include fully coupled ocean and are designed to represent observed radiative forcings over the historical period whereas future projections use two representative concentration pathways (RCPs): RCP4.5 and RCP8.5. The RCPs comprise scenarios of future changes in greenhouse gas emissions and short-lived species, as well as land-use change, used as a basis for assessing possible climate impacts (van Vuuren et al. 2011; Thomson et al. 2011). RCP4.5 is considered an intermediate mitigation scenario, with emissions peaking around 2040, and radiative forcing stabilizing at 4.5 $W m^{-2}$ at 2100, whereas RCP8.5 is a high-emissions scenario, with emissions rising throughout the twenty-first century, leading to a radiative forcing of 8.5 $W m^{-2}$ at 2100 (van Vuuren et al. 2011; Thomson et al. 2011; Riahi et al. 2011). These two scenarios were chosen to span a range of medium- to high-emissions future projections. Models were chosen based on the availability of daily rainfall data for the required periods from the British Atmospheric Data Centre (BADC). Table S1 in the online supplemental material contains a full list of model names, names of institutes, and horizontal resolutions. Because different models have different numbers of ensemble members, and because of the small number of available ensemble members, only the first ensemble member (r1i1p1) are used.

Trends from the CMIP5 simulations are compared with those from the atmosphere-only simulations from the Atmospheric Model Intercomparison Project (AMIP); daily rainfall from 28 model simulations over 1979–2008 was utilized [see Table S1 in Dunning et al. (2017) for a full list of models used].

To produce the multimodel means data were regridded using bilinear interpolation to a $1° \times 1°$ grid. For time series, variables were averaged over the domain used and no interpolation was applied.

To investigate dynamical aspects of changes [Saharan heat low (SHL) strength index and Angola low (AL) index] monthly geopotential height data (at 850 and 925 hPa) was obtained for the 29 CMIP5 models for the historical simulation over 1980–2099 and the RCP4.5 and RCP8.5 simulations over 2080–99. Other variables were also obtained from BADC, including surface temperature, 850-hPa temperature (used for calculation of potential temperature), mean pressure at sea level, and relative humidity, specific humidity, and u and v winds at 925 hPa for the same scenarios and periods.

Dunning et al. (2017) examined the representation of African rainfall seasonality in CMIP5 models, using the same method for categorizing seasonal regimes and calculating onset and cessation dates as is used here. The main biases identified include timing biases over the Horn of Africa and an overestimation of the areal extent of the winter rainfall regime over southwestern Africa. Furthermore, Dunning et al. (2017) found that the coupled simulations failed to capture the biannual regime over the southern West African coastline. However, for the most part Dunning et al. (2017) reported that coupled climate models capture the observed patterns of seasonal progression and give onset and cessation dates within 18 days of the observational dates, and thus can be used to produce projections of changing seasonality.

To compare trends in AMIP and CMIP5 simulations with observed trends, a reference dataset was required. TAMSATv3 (Tropical Applications of Meteorology using Satellite Data and Ground-Based Observations, version 3) daily rainfall estimates are produced using thermal infrared imagery (TIR) from Meteosat (provided by the European Organisation for the Exploitation of Meteorological Satellites) (Schmetz et al. 2002). Rainfall estimates are calculated using a time-invariant calibration, based on rainfall observations from a consistent rain gauge network (Tarnavsky et al. 2014; Maidment et al. 2014, 2017). The temporal consistency of both the gauge measurements used and the calibration, as well as the long time coverage (1983 onward), makes this dataset suitable for analysis of trends. Datasets that merge in rain gauge observations are not suitable, as the changing rain gauge coverage can result in spurious rainfall trends (Maidment et al. 2015). Rainfall data from TAMSATv3 were used for 1984–2016 and bilinearly interpolated to a $1° \times 1°$ grid. Other datasets were also considered; results produced using the Climate Hazards Group Infrared Precipitation with Stations (CHIRPS) daily precipitation dataset (Funk et al. 2015) are included in the online supplemental information for comparison. For the identification of the position of the tropical rain belt daily rainfall data over land and ocean were required, and thus daily precipitation

data from the Global Precipitation Climatology Project (GPCP) were used over 1997–2014 (at 1° × 1° resolution; Huffman et al. 2001).

b. *Methodology for identifying onset and cessation of rainfall seasons*

Onset and cessation dates were calculated using the methodology of Dunning et al. (2016), which extends the methodology of Liebmann et al. (2012). For analysis of changes in onset and cessation dates the method is applied separately to the three time periods used (recent period, mid-twenty-first century, and end of the twenty-first century).

The method has three stages; full details of the method can be found in Dunning et al. (2016). First, the seasonal regime at each grid point is categorized as being a dominantly annual regime (one wet season per year) or biannual regime (two wet seasons per year). This is achieved by computing the ratio of the amplitude of the second harmonic to the first harmonic. Next, in order to account for wet seasons that span the end of the calendar year, the period of the year when the wet season occurs, termed the climatological water season, is determined by identifying the minima and maxima in the climatological cumulative daily mean rainfall anomaly. The climatological cumulative daily mean rainfall anomaly is calculated by first computing the climatological mean rainfall for each day of the calendar year Q_i and the long-term climatological daily mean rainfall $\overline{Q}$. Using this, the climatological cumulative daily rainfall anomaly on day d is

$$C(d) = \sum_{i=1\text{Jan}}^{d} Q_i - \overline{Q}, \tag{1}$$

where i ranges from 1 January to the day d for which the calculation applies. The minima and maxima in C are used to define the beginning and end of the climatological water season. For locations with a biannual regime the method extension presented in Dunning et al. (2016), not included in the original method of Liebmann et al. (2012), is used to identify the climatological period of the two wet seasons. Finally, onset and cessation dates are calculated for each season and year individually. The daily cumulative rainfall anomaly is computed for each season; onset is defined as the minima in the daily cumulative rainfall anomaly and cessation is defined as the maxima. The period between the minima and maxima is a period when the rainfall is persistent in occurrence, duration, and intensity (Diaconescu et al. 2015). Because of seasons spanning the end of the calendar year, onset and cessation dates are not calculated for the first or last years of each dataset.

To produce the time series over 1950–2090 the method was modified. The original method does the annual/biannual categorization over the entire period and also determines the timing of the climatological water season (the period of the year when the wet season occurs) over the entire period. While this is suitable for 20-yr periods, it is not suitable for a 140-yr period in which we may expect shifts in the seasonal cycle. To overcome the issue of changing annual/biannual categorization, maps were produced showing regions where models showed a change in annual/biannual categorization (Fig. S3). The West Africa (7°–13°N, 10°W–9°E) and southern Africa (10°–20°S, 20°–35°E) regions for time series were chosen such that almost no models showed a change in regime (Fig. S3). The central Africa region was chosen to cover the area that showed a large increase in wet season rainfall, with a few models showing a change in regime. The multimodel-mean annual seasonal cycle over the region exhibits an annual regime for both 1980–99 (historical simulation) and 2080–99 (RCP8.5) and thus it was deemed that an annual regime could be assumed for the entire time period over this region (Fig. S3). For the Horn of Africa region (land points within 3°S–12°N, 35°–51°E) a biannual seasonal regime was assumed and the two-season method was used. If the method could not identify two wet seasons per year then the point was excluded for that year.

The second issue, that of the timing of the climatological water season (period of the year when the wet season occurs), was resolved by determining the period of the climatological water season for each year individually, using a 20-yr period centered on the year in question. For example, for 1950, daily rainfall data from 1940–59 were used to determine the beginning and end of the climatological water season. Onset and cessation dates were then calculated in the same way as described above. This adjustment should take into account any shifts in timing of the wet season.

This onset–cessation methodology identifies the period when the rainfall is persistent in occurrence, duration, and intensity relative to the mean climate (Diaconescu et al. 2015) and has been used in a number of studies (Boyard-Micheau et al. 2013; Diaconescu et al. 2015; Monerie et al. 2016; Liebmann et al. 2017). The lack of dependence on a particular threshold facilitates the production of contemporaneous onset and cessation dates across datasets with contrasting rainfall biases (Liebmann et al. 2012; Dunning et al. 2016), enabling application to climate model simulations without the need for bias correction (Dunning et al. 2017) as the cumulative rainfall anomaly is calculated separately for each model and grid point. However, because it is a

relative measure a systematic increase in rainfall will lead to no change in onset/cessation dates, whereas using methods based on exceeding a rainfall threshold (e.g., Marteau et al. 2009; Issa Lélé and Lamb 2010) would show a change in onset and cessation. Such methods, however, cannot be applied to climate model output, due to biases in both rainfall amount and occurrence, rendering useless methods that look for, for example, "no dry spell of 7 days in the next 20 days." This justified applying the cumulative rainfall anomaly method of Dunning et al. (2016), following on from Liebmann et al. (2012), which identifies changes in timing of the most persistent period of rainfall. While this method was shown to have good agreement with local indigenous methods for the present climate (Dunning et al. 2016), the same cannot be assumed for future climates. However, shifts in the timing of the periods of persistent rainfall are likely to relate to changes in timing of agricultural wet seasons, and identifying the wettest periods allows us to look at changes in physical drivers leading to these changes. The aliasing of changes in rainfall amount into changes in onset and cessation should be taken into consideration, and seasonal cycles were checked to ensure that the changes were realistic.

Frequency and occurrence of rainfall within the wet season is also investigated. A threshold of 1 mm day^{-1} was used to define a rainy day (also used in CLIMDEX indices; see https://www.climdex.org/indices.html); for each year and model the number of days over this threshold within the wet season (between onset and cessation) was counted, and the rainfall on these days was averaged to give the number of rainy days and average rainfall per rainy day, respectively. While some models (in particular those with higher spatial resolution; Zhang et al. 2016) may give more realistic current distributions and future changes in the frequency and occurrence of rainfall within the wet season, we have used all of the 29 CMIP5 models used in this study to produce these metrics, as present performance does not necessarily translate into more reliable future projections (Rowell et al. 2016) and extensive model evaluation would be required in order to justify the exclusion of models.

c. Characterization of dynamical drivers

To assess changes in the seasonal progression of the tropical rain belt, a method for defining the location of the intertropical convergence zone (ITCZ) in terms of the peak rainfall was used (Shonk et al. 2018). First, the mean daily rainfall is computed for each day of the year at each grid point. Only the region between 30°N and 30°S is considered. For each longitude and day the range of latitudes where the rainfall is greater than half of the maximum rainfall rate is considered; within this range the latitude of the rainfall centroid is taken to be the mean location of the ITCZ/tropical rain belt. Two other definitions were also used in the analysis to establish robustness (see the online supplemental information): the latitude of the maximum rainfall for each longitude and the latitude of the rainfall centroid (not limited to top 50%). Shonk et al. (2018) found that the definition based on the rainfall centroid of the top 50% gave a smoothly varying quantity, whereas the method based on maximum rainfall can exhibit large variations. Similar methods were also used by d'Orgeval et al. (2006) and Monerie et al. (2013) to analyze changes in progression of rain belts across Africa.

The SHL and AL are important drivers of rainfall seasonality and variability over West Africa and the wider Sahel (Lavaysse et al. 2009) and southern Africa (Munday and Washington 2017) respectively. An index was required for quantifying the strength of the SHL and AL to establish whether changes in the strength of the SHL or AL will influence changing seasonality. Munday and Washington (2017) identified the AL as the lowest 5% of DJF mean geopotential height (at 850 hPa) over southern Africa (0°–35°S, 5°–55°E). The strength of the AL is defined as the mean geopotential height within this mask, with lower geopotential height values indicating a stronger AL. Lower-level atmospheric thickness is commonly used to determine the location and strength of the SHL (Lavaysse et al. 2009); Dixon et al. (2017, 2018) identified the location of the SHL to be where the low-level atmospheric thickness (925–700 hPa) is greater than a 90% threshold over West Africa (0°–40°N, 20°W–30°E). The value of the 90% detection threshold quantifies the strength of the SHL; a higher value indicates higher temperatures and a stronger SHL. With future climate change we expect increasing lower tropospheric temperatures, resulting in higher lower-level atmospheric thickness (implying a stronger SHL) and higher geopotential height (implying a weaker AL). Therefore, in order to compare the changing strengths of the SHL and AL, using a metric that takes into account background changes in the meteorological variable used and uses the same variable to determine the strength of the SHL and AL would be more suitable.

An alternative methodology has been utilized by Biasutti et al. (2009) and Dixon et al. (2017) for quantifying the strength of the SHL: comparing low-level geopotential heights averaged across the Sahara (20°–30°N, 10°W–35°E) with the average geopotential height across the entire tropics (20°S–20°N). This comparison gives a climatological index of the local regional

monsoon circulation, and in the summer months describes the strength of the SHL, while also accounting for background/large-scale changes in geopotential height. Dixon et al. (2017) found strong correlation between this index and the index based on lower-level atmospheric thickness in July–September. Here we used 15°–30°N, 15°W–30°E instead, to exclude the boreal summer low over Saudi Arabia and ensure that the region contained the SHL in the boreal summer months. A similar region was defined over southern Africa, where Munday and Washington (2017) identified the AL to be 8°–30°S,10°–35°E and compared with the average geopotential height across the entire tropics (20°S–20°N) to give an index for the AL. The methods of Lavaysse et al. (2009) and Munday and Washington (2017) were used to establish the location of the SHL and AL in present and future climates; as both features are strongly constrained by topography (Chauvin et al. 2010; Evan et al. 2015; Munday and Washington 2017; Howard and Washington 2018), no large shifts in location are expected and thus such metrics can be utilized (see the online supplemental information).

Biasutti et al. (2009) and Dixon et al. (2017) used geopotential height at 925 hPa for the SHL while Munday and Washington (2017) used 850 hPa for the AL due to lower levels intersecting with topography in some CMIP5 models. Here the geopotential height at 925 hPa was used for the SHL and the 850-hPa geopotential height was used for the AL. The supplemental information includes results for both 850- and 925-hPa geopotential height for both regions and consistent results were obtained (Figs. S16 and S17). Dixon et al. (2017) noted that this metric describes the strength of the regional monsoon circulation, and only describes the strength of the low during the summer months when the low is within the regions defined; when discussing results the distinction between the strength of the regional monsoon circulation and strengths of the SHL and AL will be noted.

3. Changing rainfall seasonality and characteristics

Figure 1 shows the median change in onset, cessation, wet season length, and seasonal rainfall from 1980–99 to 2080–99 (RCP8.5 scenario) across 29 CMIP5 models. For the RCP4.5 scenario, a midrange scenario with a smaller climate change signal than RCP8.5, consistent spatial patterns of change were found, although generally of smaller magnitude (see online supplemental information). Spatial patterns were also consistent for the midcentury period, though changes were very small (results not shown). Wet season onset is projected to get later across much of West Africa and the southern Sahel, and over a northwest–southeast-oriented strip across southern Africa, with the largest changes of over 12 days on average over parts of Angola, Zimbabwe, and Mozambique (8 days for RCP4.5). West of 0°W, and at all longitudes between 10°N and 20°S, more than 75% of the CMIP models used agree that the onset will get later. In regions with an annual regime (0°–20°N), Fig. 1b shows cessation of the wet season getting later, which combined with Fig. 1a indicates that the wet season over West Africa and the Sahel is shifting later in the calendar year, with little change in length, as confirmed in Fig. 1c. Across West Africa and the Sahel, there is good model agreement (>75% of models) that cessation will get later. This is consistent with the increase in late wet season rainfall found in other studies (Biasutti and Sobel 2009; Biasutti 2013; Seth et al. 2013; Monerie et al. 2016). Sylla et al. (2015) found the largest reduction in rainfall in the premonsoon and mature monsoon phase west of 5°W and Monerie et al. (2017) also found a decrease in precipitation over the western Sahel; this is in agreement with the largest delay in onset west of 0°–5°W presented in Fig. 1a. Cook and Vizy (2012) found a reduction in the number of growing season days west of 0°W associated with a delay in onset, where Fig. 1 also shows onset getting later and a reduction in season length; however, Cook and Vizy (2012) also found increases in spring rainfall to the east of this, with an earlier onset, not found in this study or others (Biasutti and Sobel 2009; Lee and Wang 2014; Seth et al. 2013; Sylla et al. 2015). Across West Africa and the Sahel they find delays in the end date of 8–10 days on average, in agreement with the results in Fig. 1. Dunning et al. (2017) found that the coupled CMIP5 models did not capture the correct seasonal regime over the southern West African coastline, and thus results there should be viewed with caution.

Over southern Africa, the later onset results in a shorter wet season, with a reduction in total wet season rainfall centered on the Angola–Namibia–Botswana–Zambia border, with more than 75% of the models agreeing on a reduction in rainfall. Similarly, Cook and Vizy (2012) found a reduction in growing season days across Angola and southern Democratic Republic of the Congo associated with a decline in austral spring rainfall leading to a later onset. Figure 1b shows earlier cessation over Namibia and Botswana, but very few models indicate a statistically significant change here. Shongwe et al. (2009) also identified a decline in austral spring rainfall over Mozambique and Zimbabwe, which they associated with a delay in the onset. To the north of the equator, in central regions, wet season rainfall is projected to increase, with strong model consensus and the largest statistically significant changes found over

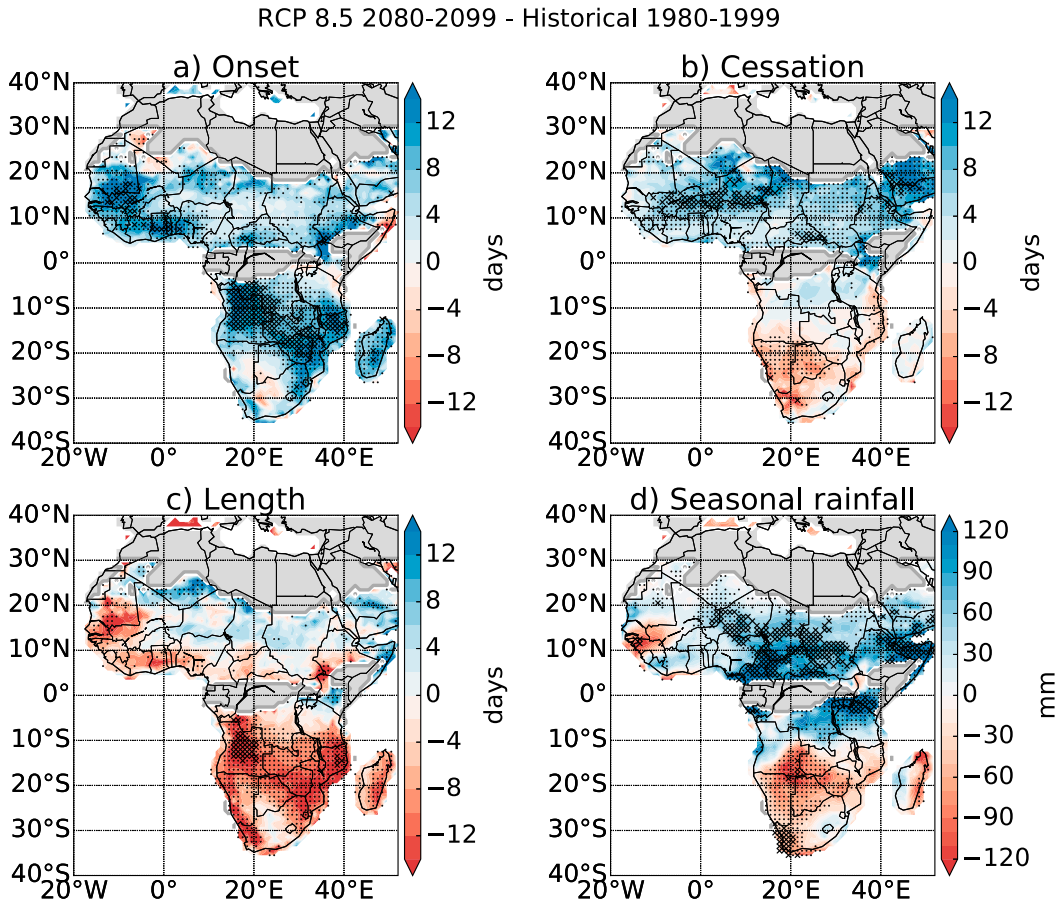

FIG. 1. Median change in (a) onset, (b) cessation, (c) season length, and (d) wet season rainfall in 29 CMIP5 simulations from 1980–99 (historical simulation) to 2080–99 (RCP8.5 scenario). Blue colors indicate the onset/cessation getting later while red colors indicate onset/cessation getting earlier. Crosses indicate where 75% of the simulations agree on the sign of the change, and more than 50% of the models show a statistically significant change (Mann Whitney *U* test, 5% significance level). Dots indicate where 75% of the simulations agree on the sign of the change. Gray regions indicate regions where fewer than five models produce onset/cessation dates due to a dry climate or two wet seasons per year.

Cameroon, southern Chad, and the surrounding regions, with average increases greater than 75 mm over 5°–11°N, 15°–30°E, (50 mm for RCP4.5), also found by Cook and Vizy (2012). Little change in total wet season rainfall is found west of 5°E. Over northern Tanzania there is little change in seasonal timing but there is an increase in total wet season rainfall.

The central equatorial region and Horn of Africa experience two wet seasons per year; projections for the "long rains" (boreal spring wet season) and "short rains" (boreal autumn wet season) are shown in Fig. 2. Earlier cessation of the long rains and later onset of the short rains implies a longer boreal summer dry season; however, these changes are less than a week on average and only statistically significant over small areas. The most notable changes are for the short rains; Figs. 2d and 2h show the end of the short rains occurring over 8 days later on average (similar value for RCP4.5) and substantial increases in rainfall amount, similar to the findings in Shongwe et al. (2011) and Cook and Vizy (2012). There is strong model consensus, with more than 75% of the models agreeing on later cessation and heavier rainfall across the region. Coupled climate simulations for the historical period overestimate the short rains and underestimate the long rains relative to observations, and thus projections of increasing short rains should be viewed with caution (Tierney et al. 2015; Yang et al. 2015b; Dunning et al. 2017). The pattern of surface warming in the Indian Ocean shows greater warming in the northwest Indian Ocean compared to the southeast Indian Ocean (Zheng et al. 2013), implying an increasingly positive Indian Ocean dipole (IOD) (results not shown). A positive IOD leads to increased rainfall over East Africa, particularly during the short

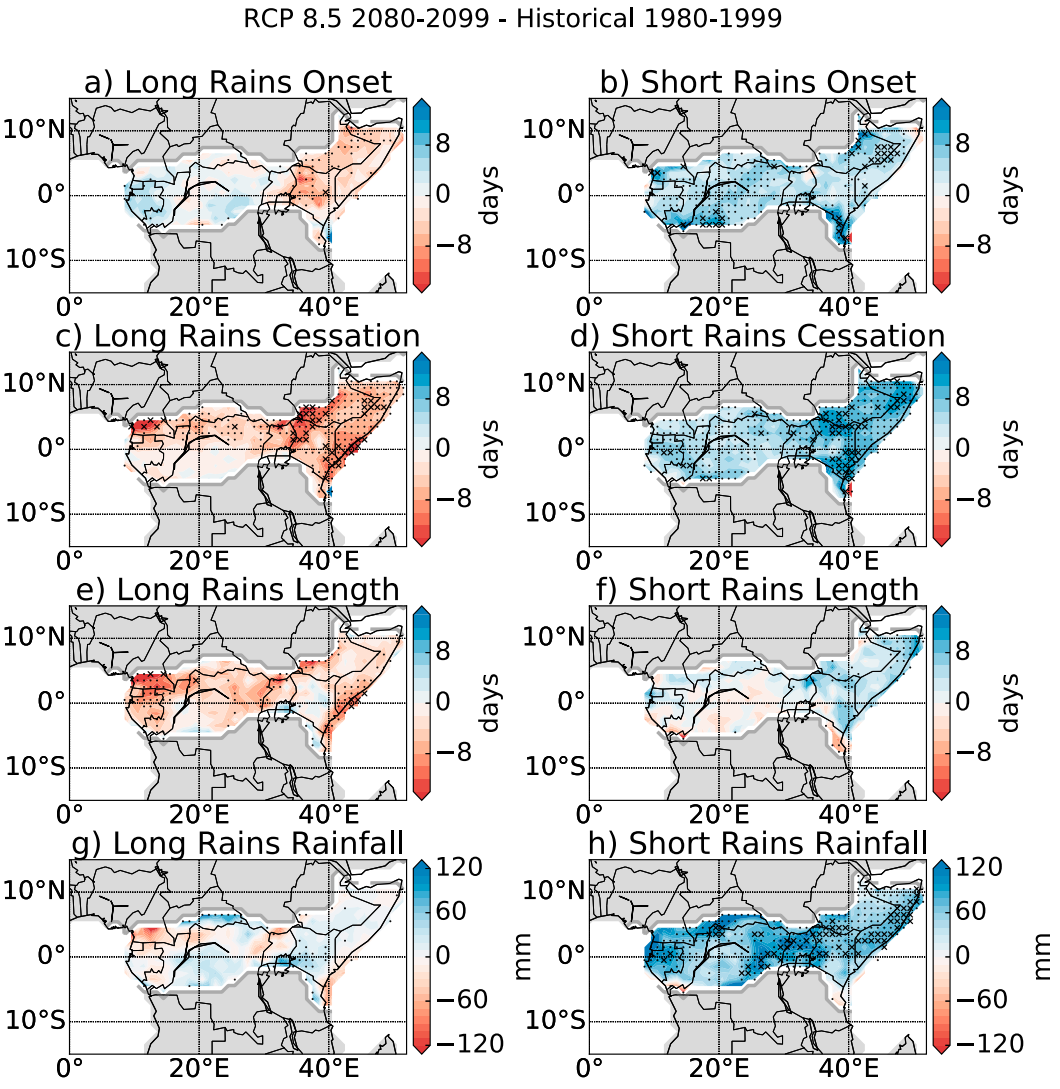

FIG. 2. Median change in (a),(b) onset, (c),(d) cessation, (e),(f) season length, and (g),(h) wet season rainfall for the (left) long rains (boreal spring) and (right) short rains (boreal autumn) in 29 CMIP5 simulations from 1980–99 (historical simulation) to 2080–99 (RCP8.5 scenario). Blue colors indicate the onset/cessation getting later while red colors indicate onset/cessation getting earlier. Crosses indicate where 75% of the simulations agree on the sign of the change, and more than 50% of the models show a statistically significant change (Mann Whitney *U* test, 5% significance level). Dots indicate where 75% of the simulations agree on the sign of the change. Gray regions indicate regions where fewer than five models produce onset/cessation dates due to a dry climate or one wet season per year.

rains (Black et al. 2003; Shongwe et al. 2011), which may contribute to the longer and wetter short rains in Fig. 2. Farther south, Funk et al. (2008) found that warming of the Indian Ocean disrupted onshore moisture transports leading to reduced growing season rainfall over southeast Africa. Shongwe et al. (2009) also found a substantial weakening of moisture transport from the Indian Ocean along the southeast coast of southern Africa, related to reduced austral spring rainfall and a later onset. Thus, the pattern of warming in the Indian Ocean may enhance the short rains over the Horn of Africa (Fig. 2) and lead to later onset and reduced rainfall over southern Africa (Fig. 1). However, Lazenby et al. (2018) did not find sufficient evidence of a link between changing OND rainfall over southern Africa and changing SST gradients.

In addition to the onset and cessation, the manner in which precipitation occurs also impacts agriculturalists and other stakeholders. Long dry periods can reduce soil moisture and harden the surface layer; thus, when heavy

rainfall events do occur a smaller fraction infiltrates into the root layer and increased runoff leads to soil erosion (Black et al. 2016). Additionally, heavy rainfall can adversely affect crops such as coffee and cocoa, where intense rainfall may lead to the damage of the flowers (Rosenthal 2011; Frank et al. 2011; Hutchins et al. 2015). Figure 3 shows the change in average rainfall per rainy day and number of rainy days in the wet season (where a rainy day is any day with rainfall $\geq$1 mm during the wet season), in addition to changes in onset and total wet season rainfall over part of southern Africa (10°–20°S, 20°–35°E). While there is only a small change in total seasonal rainfall (Fig. 3b), there is a significant decrease in the number of rainy days (10 fewer days per wet season on average in 2090 compared to 1980–2000) and increase in the average rainfall per rainy day (increase of $>$0.75 mm day^{-1} on average in 2090 compared to 1980–2000; Figs. 3c,d). Similarly, Sillmann et al. (2013) found a decline in the number of heavy precipitation days, with more consecutive dry days and a higher percentage of rainfall coming from very wet days over this region. The observations exhibit much interannual variability, with none of the trends statistically significant at the 5% level (Wald test, with the null hypothesis that the slope is zero). Over 1985–2007, time series from TAMSATv3 and the coupled simulations all show increasing rainfall per rainy day (TAMSATv3; 0.30 mm day^{-1} decade^{-1}), in agreement with future trends. Although overall there is a slight increase in the number of rainy days, there are large interannual variations. Precipitation estimates based on infrared radiation, such as TAMSATv3, do not capture daily extremes well and so may not simulate this aspect of climate change accurately (Maidment et al. 2014, 2017). Similar patterns of increasing intensity under future climate change are found over West Africa (7°–13°N, 10°W–9°E; Fig. S4), with increasing rainfall per rainy day over 1985–2007 in TAMSATv3, AMIP, and the coupled simulations, with trends ranging from 0.09 to 0.12 mm day^{-1} decade^{-1}, and future projections of decreasing numbers of rainy days, with decreases of 5–10 rainy days on average in 2090 compared to 1980–2000. Taylor et al. (2017) identified an increase in the frequency of intense storms over the Sahel since 1982, associated with Saharan warming and an increased meridional temperature gradient. Increasing rainfall per rainy day may explain the non–statistically significant change in rainfall over Mauritania and Senegal (Fig. 1d), despite the statistically significant reduction in season length (Fig. 1c), associated with the later onset (Fig. 1a). central Africa (5°–11°N, 15°–30°E) exhibits increasing average rainfall per day, both over the observational and future periods, and little long-term change in number of rainy days (Fig. S5), consistent with the increase in seasonal rainfall shown in Fig. 1d. Other studies have identified similar trends over southern Africa (Sylla et al. 2015; Pohl et al. 2017) and at wider scales (Cubasch et al. 2001); here we have identified that the same changes occur within the wet season, with the change in number of rainy days potentially important for determining changes in overall seasonal rainfall.

Figure 4 shows the observed and projected changes in cessation of the wet season over West Africa (7°–13°N, 10°W–9°E) and central Africa (5°–11°N, 15°–30°E), and cessation of the short rains (boreal autumn wet season over the Horn of Africa; land points in 3°S–12°N, 35°–51°E). Dunning et al. (2016) showed that the cessation of the short rains follows on from the cessation of the main wet season over West Africa and the Sahel, associated with the southward retreat of the rain belt in boreal autumn. The projections indicate cessation shifting later in all three regions in the future with multimodel mean changes of up to 10 days (Fig. 4). Observed trends from TAMSATv3 and AMIP simulations also show cessation getting later, with particularly strong trends in TAMSATv3 over the central Africa region, with trends of around 5 days decade^{-1} over 1985–2007 (Fig. 4b). Agreement among future projections, AMIP, and observed trends adds credence to future projections.

Time series for the West African region shows the best AMIP–TAMSATv3 agreement compared to the other regions with trends of 1.8 and 2.5 days decade^{-1}, respectively, over 1985–2007. Some of this trend is likely to be attributable to the recent rainfall recovery over the Sahel region, following the devastating drought in the 1980s (Biasutti et al. 2009; Nicholson 2013; Evan et al. 2015), but it is also strongly influenced by decadal climate variability (Maidment et al. 2015). Figure 4c shows cessation of the short rains getting later by 4.2 days decade^{-1} over 1985–2007 (TAMSATv3), with much interannual variability. Agreement of future projections with past trends may add additional confidence to future projections; although the trends in TAMSATv3 and AMIP are larger than those from the coupled simulations in all three regions, they are more likely to reflect internal climate variability not represented by ensemble mean simulations.

In summary, CMIP5 projections show changes in the seasonal timing of the wet season over Africa. A delay in the wet season is projected over West Africa and the Sahel, with recent trends showing the cessation of the wet season getting later. Over southern Africa a later onset results in a shorter wet season, and reduced total wet season rainfall. Increasing rainfall is projected for the short rains over the Horn of Africa, with a later end to the season. Model agreement, with $>$75% of the

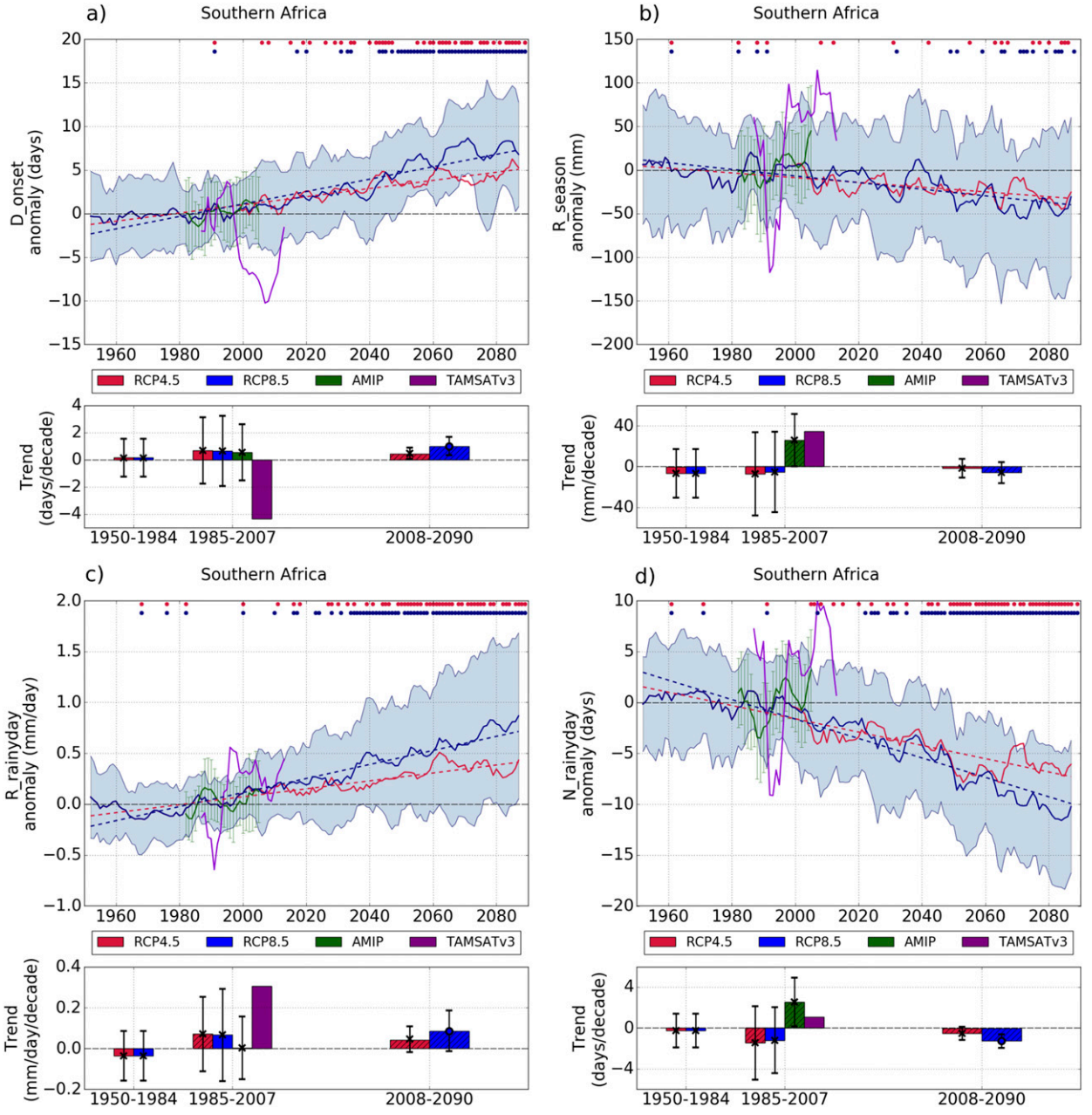

FIG. 3. Time series of (a) onset, (b) total wet season rainfall, (c) average rainfall per wet season rainy day (≥1 mm), and (d) number of rainy days (≥1 mm) in the wet season over a region in southern Africa (10°–20°S, 20°–35°E). The red and blue lines are the multimodel mean (from 29 CMIP5 models) after a 5-yr running mean was applied for RCP4.5 and RCP8.5, respectively, over 1950–2090. The blue shaded area indicates the spread of model projections (plus and minus one standard deviation for RCP8.5 simulations; the spread for RCP4.5 was similar). The green line (with error bars) is the multimodel mean (plus and minus one standard deviation) for the AMIP simulations (1979–2008). The purple line is produced using TAMSATv3 precipitation (1985–2015). The dots indicate when the range of values from 29 models for that year is significantly different from the range for 1980–2000 at the 5% level, using a Mann–Whitney U and *t* test. The bar charts indicate the trend over different periods: 1950–84, 1985–2007 (AMIP and observations period), and 2008–90. The height of the bars indicates the trend of the multimodel mean; hatching indicates the trend is significantly different from 0 at the 5% level (Wald test). The circle/cross and error bar indicate the mean and standard deviations of the trend from the 29 models; a circle indicates over 50% of the models show a trend significantly different from 0 at the 5% level. Multimodel mean time series are computed after a 5-yr moving average has been applied, and a 5-yr moving average is also applied to the observation time series; trends are computed using the unsmoothed data.

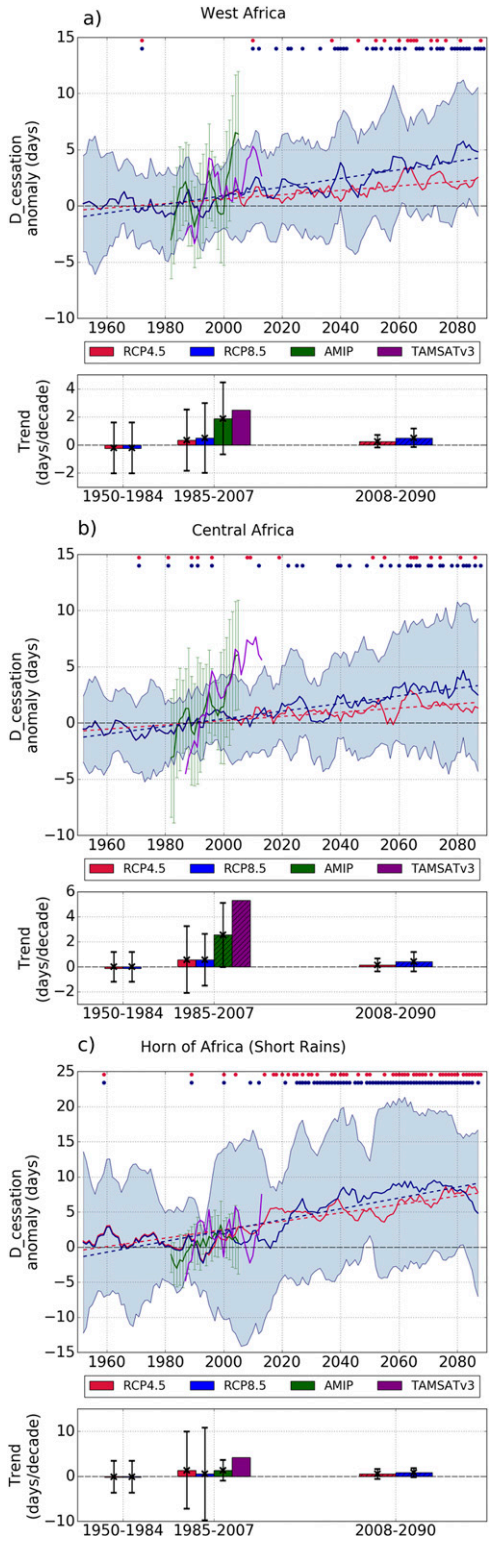

FIG. 4. As in Fig. 3, but for cessation over regions in (a) West Africa (7°–13°N, 10°W–9°E) and (b) central Africa (5°–11°N, 15°–30°E) that experience one wet season per year, and (c) cessation of the short rains over the Horn of Africa (land points within 3°S–12°N, 35°–51°E,).

models agreeing on the sign of the change, indicates robustness, and agreement with observations and AMIP adds credence. Within the wet season average rainfall per rainy day is projected to increase, while the number of rainy days is projected to decline in regions of stable or declining rainfall and remain constant in central Africa, where rainfall is projected to increase. In the next section possible drivers of such changes will be explored.

4. Links between the Saharan heat low, the Angola low, and later onset/cessation of wet seasons

The seasonal progression of rainfall over Africa is driven by complex interaction of a number of factors (Nicholson 2000; Sultan and Janicot 2003; Lavaysse et al. 2009; Nicholson 2013; Lazenby et al. 2016; Munday and Washington 2017; Nicholson 2017). In this section links between the seasonal progression of the tropical rain belt and the strength of the Angola low and Saharan heat low are explored.

The northward and southward progression of the tropical rain belt, following the maximum incoming solar radiation, is one of the major drivers of the seasonal cycle of precipitation across Africa. The Saharan heat low and Angola low form over northern and southern Africa, respectively, during the local summer, and cyclonic circulation associated with these features leads to significant transport of moisture onto the continent from the neighboring oceans (Nicholson 2013; Lazenby et al. 2016). Comparing responses across the ensemble of CMIP5 models, and inspecting outliers, enables us to utilize the CMIP5 ensemble as a ''test bed'' to examine mechanistic hypotheses.

The trend of later cessation over West Africa and the Sahel and onset getting later over southern Africa, combined with the later shift of the short rains, suggests a change in the progression of the tropical rain belt during the second half of the calendar year. Separate studies have identified factors suggesting both the later shift of cessation over the Sahel (Biasutti and Sobel 2009; Seth et al. 2013; Monerie et al. 2016) and the later onset over southeast Africa (Shongwe et al. 2009). Biasutti and Sobel (2009) associated a delay in the seasonal cycle of precipitation with changes in the SST seasonal cycle. Seth et al. (2013) found a redistribution of monsoon rainfall from early to late in the monsoon season, with a reduction in early season rainfall being the consequence of an enhanced convective barrier resulting from reduced moisture availability. Dwyer et al. (2014) found a global amplification and phase delay of the seasonal cycle of precipitation, with the delay attributed to changes in the seasonality of the circulation. In this section we investigate factors affecting the delay in the cessation

over West Africa and the Sahel and onset over southern Africa.

a. Background on SHL and AL

During the boreal summer high insolation and low evaporation over the Sahara leads to the formation of an intense heat low (Lavaysse et al. 2009; Dixon et al. 2017), termed the Saharan heat low, with high surface temperatures and low surface pressures (Lavaysse et al. 2009; Parker and Diop-Kane 2017). The associated cyclonic circulation increases the northeasterly Harmattan flow and southwesterly monsoon flow (Lavaysse et al. 2009; Nicholson 2013; Parker and Diop-Kane 2017) that transports moisture rich air into the Sahel region, fueling convection and precipitation (Dixon et al. 2018), and thus forms a key part of the West African monsoon (Chauvin et al. 2010; Nicholson 2013). Variations in both the strength and position of the SHL have been shown to affect the onset of the monsoon and total seasonal rainfall (Lavaysse et al. 2009; Biasutti and Sobel 2009; Chauvin et al. 2010; Park et al. 2016; Dixon et al. 2017) as well as intraseasonal variations, including monsoon "bursts" (Nicholson 2013; Parker and Diop-Kane 2017). Furthermore, Chauvin et al. (2010) found that intraseasonal variability of the SHL was associated with midlatitude intraseasonal variability.

Future projections indicate strengthening and deepening of the SHL leading to increasing Sahel rainfall (Biasutti and Sobel 2009; Monerie et al. 2016; Vizy and Cook 2017). Enhanced temperatures over the Sahara act to deepen the SHL and enhance monsoon flow, bringing more moisture into the region. Water vapor is a greenhouse gas, leading to further temperature increases (Evan et al. 2015; Vizy and Cook 2017). Variations in dust aerosol have also been linked with variations in the strength of the SHL (Alamirew et al. 2018) and Sahel precipitation (Konare et al. 2008; Solmon et al. 2008).

The Angola low forms over a plateau region in the southern Angola–northern Namibia area in austral summer, at the southern limit of a trough of low pressure extending from Ethiopia, through central Africa, associated with the intertropical convergence zone (Reason et al. 2006; Munday and Washington 2017). Variations in the strength of the AL have been associated with both daily (Crétat et al. 2018) and interannual precipitation variability (Cook et al. 2004; Munday and Washington 2017) over southern Africa. Howard and Washington (2018) found that on a synoptic scale the AL can be separated into the Angola heat low and Angola tropical low, with the precipitation variability more strongly related to the interannual variability of the tropical lows. Increased westerlies from the southeast Atlantic, associated with strengthened AL circulation, increase low-level moisture in this region, increasing the formation of tropical–extratropical cloud bands and precipitation (Cook et al. 2004; Reason et al. 2006; Lazenby et al. 2016; Munday and Washington 2017). Conversely, Cook et al. (2004) found that dry late summers (January–March) were associated with a decrease in the strength of the AL.

b. Future changes in SHL and AL

Given the important role that the SHL and AL play in driving rainfall seasonality and variability over West Africa and the wider Sahel (Lavaysse et al. 2009) and southern Africa (Munday and Washington 2017; Crétat et al. 2018; Howard and Washington 2018), their influence in a changing climate was investigated. A metric based on the methodology of Biasutti et al. (2009) and Dixon et al. (2017) was used to quantify changes in the strength of the SHL and AL (see section 2). This index describes the strength of the regional circulation throughout the year; during the boreal (austral) summer it describes the strength of the SHL (AL) (Dixon et al. 2017). The locations of the two regions used to define the strengths of the SHL and AL are shown in Fig. 5, with the colors showing the multimodel mean increase in 850-hPa potential temperature over JJA (Fig. 5a) and DJF (Fig. 5b). The largest increases in temperature are found across North Africa, north of 20°N in JJA. Over the AL region a smaller increase in potential temperature is found in both JJA and DJF.

Comparison of the relative strength of the SHL and AL in the historical and future simulations shows an increase in the strength of the SHL/northern regional circulation in June–September, with the largest increases toward the end of the boreal summer (Figs. 6c,e) as found in Biasutti et al. (2009). Recent increasing greenhouse gas concentrations have been shown to act to strengthen the West African monsoon circulation and the SHL (Dong and Sutton 2015), and also storm intensity (Taylor et al. 2017), with continuing emissions likely to contribute to future strengthening. The magnitude of the increase in strength of the AL in austral summer is similar to the increase in strength of the southern regional circulation throughout the entire year and is of lower magnitude than the increase in strength of the SHL in the late boreal summer months (Figs. 6c–e). This is consistent with the increases in potential temperature seen in Fig. 5.

c. Change in the progression of the tropical rain belt

The method of Shonk et al. (2018) was used to identify the mean position of the tropical rain belt (TRB) in CMIP5 simulations (see section 2) to assess whether a change in seasonal progression of the TRB was

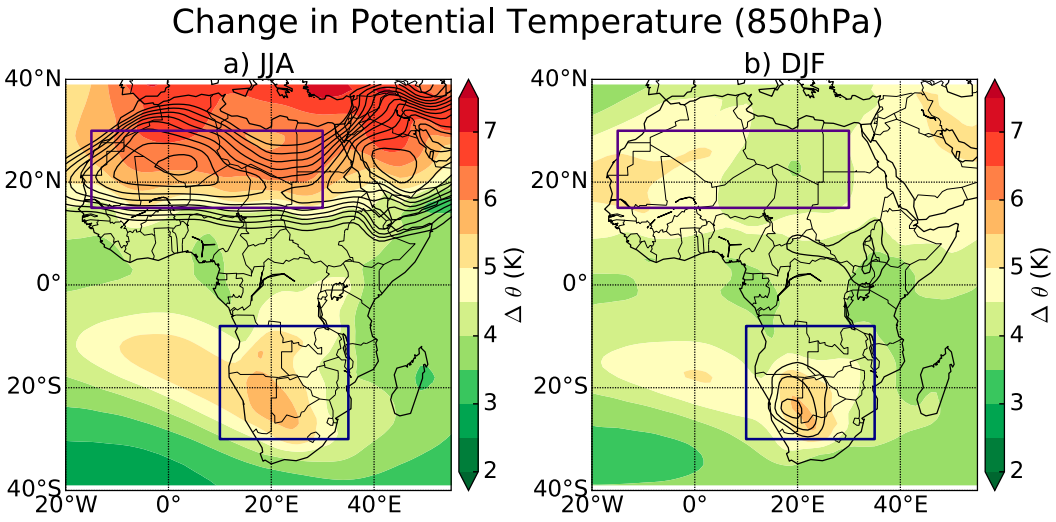

FIG. 5. Multimodel mean change in potential temperature (850 hPa) for RCP8.5 (2080–99) minus historical (1980–99) in (a) JJA and (b) DJF. Contours show the multimodel mean potential temperature (850 hPa) in the historical simulation (1980–99), increasing in steps of 1 K from 308 K. The purple (navy) boxes indicate the regions used to compute the strength of the SHL (AL).

observed. Figures 6a and 6b show the mean seasonal progression of the TRB and its response to climate change over 0°–35°E. The analysis was repeated using two other definitions for TRB (latitude of maximum rainfall and latitude of rainfall centroid with rainfall not limited to top 50%; see section 2); similar results were obtained, suggesting that the analysis is robust to TRB definition (see online supplemental information). Figure 6a demonstrates agreement between the seasonal progression of the TRB in observations and CMIP5 models; the main difference is between January and March/April. Under RCP8.5 the southward progression of the TRB shifts later in the year; the TRB is on average 0.8°–1.2° north of its position in the historical simulation from August to December. When viewed from a single latitude the passage of the TRB occurs up to 15 days later. This is consistent with the trends seen in onset and cessation (Figs. 1 and 2); a later southward progression leads to a later cessation over West Africa and later onset over southern Africa. Using similar methods, d'Orgeval et al. (2006) also found a northward shift in the location of the rain belt in October and Monerie et al. (2013) identified a northward shift from August to November, when considering the region 10°S–21°N, 0°–25°E. Analysis with an observational dataset (GPCP 1DD, as daily rainfall data over land and ocean were required; Huffman et al. 2001) confirms that later southward progression of the TRB is associated with later cessation and onset over West Africa and the Sahel and over southern Africa respectively (see online supplemental information and Fig. S11). Maidment et al. (2014) show high correlation between GPCP and TAMSAT rainfall, and Dunning et al. (2016) show good agreement between onset and cessation dates produced using TAMSAT and GPCP 1DD.

The later onset over West Africa is mostly significant west of 0° (Fig. 1). The change in position of the TRB was analyzed separately over this region. Between 0° and 16°W a southward shift in the mean position of the TRB is apparent from January to June under the RCP scenarios compared with the historical period (1980–99; see online supplemental information). This is consistent with the later onset in Fig. 1a. Other studies have linked reduced early season precipitation over West Africa with lower relative humidity resulting from reduced moisture convergence (Seth et al. 2013) related to southwesterly flow anomalies carrying more moisture to the east (Cook and Vizy 2012; see online supplemental information).

d. Links between the Saharan heat low, the Angola low, and progression of the tropical rain belt

We postulate that the increase in strength of the SHL, associated with higher surface temperatures, lower surface pressure, and lower geopotential height over the region, toward the end of the boreal summer is causing the TRB to move farther north in July and August (Figs. 6a,b). This in turn delays the southward progression, thus giving a later cessation of the wet season over West Africa and the Sahel, and is one of the factors contributing to the later short rains over the Horn of

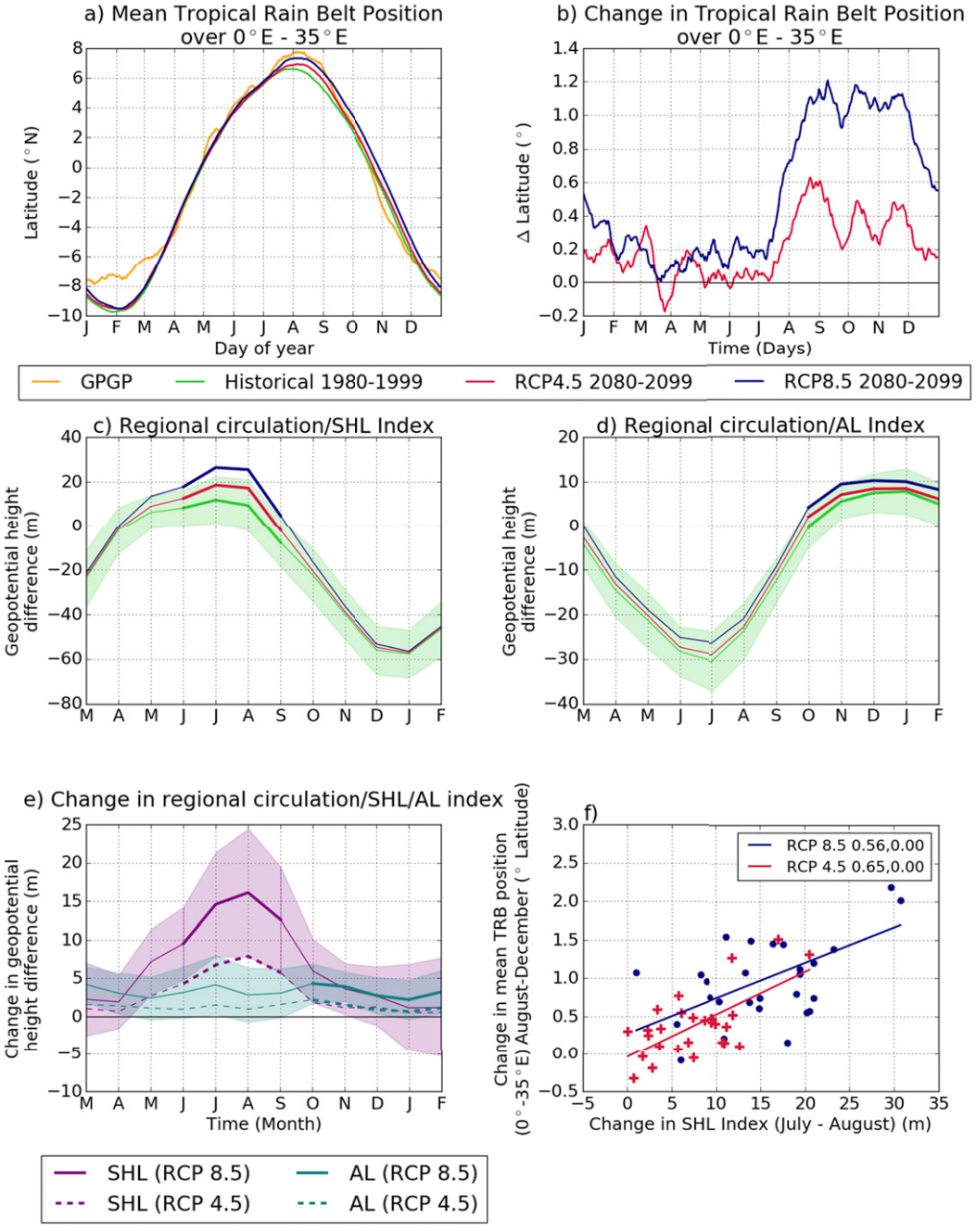

FIG. 6. (a) Mean tropical rain belt position and (b) change in position of the TRB in RCP4.5 and RCP8.5 simulations over 29 CMIP5 models for 2080–99 compared with historical values for1980–99 [and GPCP over 1997–2014 for (a)], averaged over 0°–35°E, produced using the method of Shonk et al. (2018) on a daily basis and smoothed using a 15-day running mean. Also shown is the regional circulation index for (c) the northern region (including SHL) and (d) the southern region (including AL) for the historical, RCP4.5, and RCP8.5 simulations over 29 CMIP5 models for 1980–99 and 2080–99. The green shaded area indicates the range across the 29 CMIP5 models for the historical simulation. The thicker lines indicate when the SHL or AL is within the region, and the regional circulation index also describes the strength of the SHL or AL. (e) Change in strength of the regional circulation for north/SHL (purple) and south/AL (teal) from historical values for 1980–99 to RCP4.5 (dashed) and RCP8.5 (solid) (2080–99). Again, thicker lines indicate when the SHL or AL is within the region, and the regional circulation index also describes the strength of the SHL or AL. The shading shows the model spread (plus and minus one standard deviation) for RCP8.5. (f) Mean change in position of TRB over 0°–35°E (August–December) is plotted against change in SHL index for RCP4.5 and RCP8.5; the values in the legend indicate the Pearson correlation coefficient r and the p value. EC-EARTH is excluded from (f).

Africa, and later onset of the main wet season over southern Africa. The changes associated with the strengthening of the SHL/northern regional circulation [higher surface temperatures, lower surface pressure (Fig. 7; see also Fig. S18), and lower geopotential height] toward the end of the boreal summer favor moisture convergence over the northern part of Africa. Figure 7 shows greater transport of moisture into the Sahel region, both southerly from the Gulf of Guinea and northerly from the Mediterranean (partly linked to increased moisture over the Mediterranean Sea), and northward anomalies around the equator. Monerie et al. (2016) also found a northward shift of the monsoon and increased moisture transport from the Mediterranean Sea. This is likely to be linked to later cessation over this region found in Fig. 1b. Additionally, there is less moisture transport into southern Africa, with reduced relative humidity in August–October (Fig. 7; see also Fig. S18). Seth et al. (2013) associated later onset over southern Africa with reduced boundary layer moisture availability at the end of the dry season, resulting from reduced moisture convergence and lower evaporation. Thus, changes in moisture transport associated with changes in the strength of the SHL may influence relative humidity over southern Africa and delay the start of the wet season, although other drivers, including changes in pressure and surface temperatures over the neighboring oceans, are also likely to play a role (Funk et al. 2008; Shongwe et al. 2009; Lazenby et al. 2018).

To test the hypothesis that the increase in strength of the SHL and regional circulation over North Africa toward the end of the boreal summer delays the southward progression of the TRB, the increase in strength of the SHL in 29 CMIP5 models is plotted against the mean change in TRB position (Fig. 6f). Models with a larger increase in strength of the SHL in July and August also exhibited a larger northward shift in the position of the TRB in August–December; conversely, models with a smaller amplification of the SHL such as EC-Earth have a smaller change in TRB position (Fig. 6f), with the correlation coefficient statistically significant at the 5% confidence level. In their analysis of one regional climate model, Cook and Vizy (2012) related a deepening of the SHL with increased southwesterly monsoon flow and a delay in the wet season over the Sahel; we have extended this by testing the hypothesis quantitatively across the CMIP5 ensemble. Further analysis, with targeted model simulations and analysis, is required to confirm this connection.

The limited increase in strength of the SHL under RCP8.5 in EC-Earth is potentially related to less warming over North Africa (20°–50°N, 10°W–60°E) in July–September and over the Mediterranean during

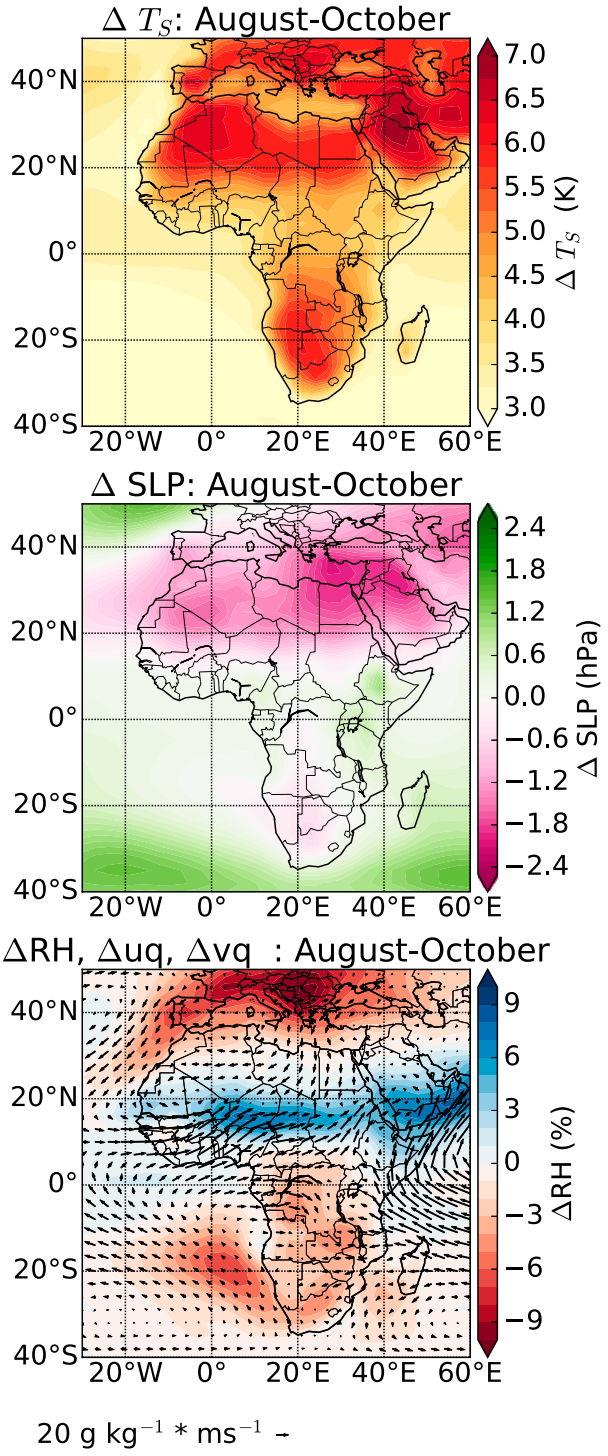

FIG. 7. Multimodel mean change in (top) surface temperature (K), (middle) sea level pressure (hPa), and (bottom) relative humidity (%) and moisture flux (g kg^{-1} m s^{-1}) at 925 hPa from 1980–99 (historical) to 2080–99 (RCP8.5 simulation) over August–October.

July and August (lowest 10% of the 29 CMIP5 models used in this analysis). Furthermore, EC-Earth also does not capture the boreal summer amplified warming over North Africa, southern Europe, the Mediterranean Sea, and central Asia compared with the global temperature increase, seen in other CMIP5 models, indicating that some of the difference may be related to the simulated amplification of the land–sea temperature contrast (Sutton et al. 2007; Joshi et al. 2008; Lambert et al. 2011).

In summary, a northward shift in the mean position of the tropical rain belt in August–December (and consequent later southward progression of the tropical rain belt) and later onset/cessation of the wet season has been identified and linked with increasing strength of the Saharan heat low. Simulations with stronger amplification of the heat low experience a greater delay in the southward progression of the tropical rain belt.

5. Conclusions

An objective methodology has been used to investigate changes in the characteristics of African wet seasons under climate change across 29 CMIP5 models. Additionally, changes in large-scale drivers of the seasonal cycle of precipitation over Africa are investigated to explore the physical mechanisms underlying future changes.

Our key findings are the following:

- A pattern of increasing rainfall intensity was identified, with higher average rainfall per rainy day found across regions of West Africa, southern Africa, and central Africa. Combined with a decline in the number of rainy days this leads to little change, or a slight decline in the total wet season rainfall over West Africa and southern Africa. Over central Africa the combination of increasing rainfall per rainy day with little change in the number of rainy days leads to increases in the total seasonal rainfall.
- Large parts of southern Africa are projected to experience a later onset date, with changes of around 12 days over Angola, as well as a shorter wet season and less wet season rainfall.
- Over the Horn of Africa, which experiences two wet seasons per year, the second wet season (‘‘short rains’’) is projected to end over a week later, with a large increase in seasonal rainfall.
- Over West Africa and the Sahel both onset and cessation are projected to get later, with the entire wet season shifting 5–10 days later in the calendar year, but with little overall change in the length of the wet season.
- The southward retreat of the tropical rain belt is projected to shift later in the calendar year, consistent with the trends of later cessation over West Africa and the Sahel, later short rains, and later onset over Southern Africa. On average the tropical rain belt is projected to be 0.8°–1.2° north of its previous position over August–December.

Large increases in surface temperature over the Sahara and North Africa during the boreal summer months lead to an intensification of the Saharan heat low. Smaller changes are identified in the strength of the Angola low. Thus it is proposed that the higher temperatures and lower surface pressure and geopotential height means that the tropical rain belt travels farther north and stays north longer, delaying the southward retreat, although other factors (including changing SST) are also likely to alter rainfall seasonality farther south. Across the 29 CMIP5 models used we found strong correlation between the increase in strength of the SHL and the shift in the TRB position, with models that had a larger increase in the strength of the SHL exhibiting a larger shift in the position of the TRB. A number of other factors may also play a role, but the analysis of these factors is beyond the scope of this study.

Previously, Cook and Vizy (2012) analyzed future projections of the growing season across Africa in a single regional climate model and proposed that delay in the wet season over the Sahel was related to the deepening of the SHL. We found consistent results when we tested the SHL–wet season delay hypothesis quantitatively across the CMIP5 ensemble.

Further analysis is required to explore intermodel differences, and the impacts of other drivers. For example, a number of studies have identified the role of warming in the western Indian Ocean on moisture transport over southern Africa (Funk et al. 2008; Shongwe et al. 2009), although Lazenby et al. (2018) found no robust link between austral spring rainfall and changing SST gradients. They commented on the potential role of South Atlantic high pressure as a driver of changing onset (Reason et al. 2006) but did not investigate this further. Seth et al. (2013) associated spring precipitation decreases across southern Africa with declining moisture convergence and reduced evaporation. In this study, we found no robust link between an increase in the strength of the Angola low and changing seasonality. Thus, investigating the role of other drivers, including pressure patterns over the South Atlantic and different patterns of Indian Ocean warming on the seasonal cycle of precipitation, would be an interesting extension. Fully understanding intermodel differences in projected

changes in the Saharan heat low would also advance this work further.

Dunning et al. (2017) identified some discrepancies in the representation of the seasonal cycle in coupled CMIP5 simulations, namely timing biases over the Horn of Africa and an overestimate of the short rains, an overestimate of the region experiencing a winter rainfall regime over southwest Africa, and an incorrect seasonal cycle over the southern West African coastline. Thus future projections for these regions should be viewed with caution. Model improvements that reduce such biases in coupled simulations are needed to produce reliable future projections over such regions.

In conclusion, future climate change will lead to a shift in the timing of wet seasons over Africa, with a delay in the wet season over West Africa and the Sahel, and later onset leading to a reduction in season length over southern Africa. This may have implications for crop development, as a shorter growing season may mean that crops do not reach full maturity. Additionally, increasing intensity of rainfall may adversely affect crops, particularly at certain times during coffee development. Further work is required to investigate additional drivers, and their interactions, as well as attribution of intermodel differences.

Acknowledgments. The authors thank two anonymous reviewers for their helpful comments.

We acknowledge the World Climate Research Programme's Working Group on Coupled Modelling, which is responsible for CMIP, and we thank the climate modeling groups (models listed in Table S1) for producing and making available their model outputs; for CMIP, the U.S. Department of Energy's PCMDI provided coordinating support and led development of software infrastructure in partnership with the Global Organization for Earth System Science Portals. Model data were sourced from the CMIP5 data portal (http://cmip-pcmdi.llnl.gov/cmip5/data_portal.html) and the British Atmospheric Data Centre (http://badc.nerc.ac.uk/).

All observational datasets exploited are publicly available datasets. The TAMSATv3 dataset is available from the TAMSAT website (http://www.met.reading.ac.uk/~tamsat/data). GPCP daily data are available from http://precip.gsfc.nasa.gov/. The CHIRPS dataset, produced by the Climate Hazards Group, is available at http://chg.geog.ucsb.edu/data/chirps/#_Data.

Caroline M. Dunning is supported with funding from a Natural Environment Research Council (NERC) Ph.D. Studentship through the SCENARIO Doctoral Training Partnership Grant NE/L002566/1. Richard P. Allan's contribution to the research leading to these results has received funding from the National Centre for Earth Observation and the European Union Seventh Framework Programme (FP7/2007-2013) under Grant Agreement 603502 (EU project DACCIWA: Dynamics–aerosol–chemistry–cloud interactions in West Africa). Emily Black's contribution to the research has been supported by the National Centre for Atmospheric Science (Climate division) ACREW project, which is supported by NERC and the Global Challenges Research Fund. She also gratefully acknowledges support from the NERC/DFID BRAVE project (NE/M008983/1), the NERC/DFID HyCristal project (NE/M020371/1), and the Global Challenges Research Fund project, SatWIN-ALERT (NE/R014116/1). We are grateful to the Mars Wrigley Confectionery research team for stimulating discussions on the wider context and applications of this work.

REFERENCES

Alamirew, N. K., M. C. Todd, C. L. Ryder, J. H. Marsham, and Y. Wang, 2018: The early summertime Saharan heat low: Sensitivity of the radiation budget and atmospheric heating to water vapour and dust aerosol. *Atmos. Chem. Phys.*, **18**, 1241–1262, https://doi.org/10.5194/acp-18-1241-2018.

Allan, R. P., B. J. Soden, V. O. John, W. Ingram, and P. Good, 2010: Current changes in tropical precipitation. *Environ. Res. Lett.*, **5**, 025205, https://doi.org/10.1088/1748-9326/5/2/025205.

Biasutti, M., 2013: Forced Sahel rainfall trends in the CMIP5 archive. *J. Geophys. Res. Atmos.*, **118**, 1613–1623, https://doi.org/10.1002/jgrd.50206.

——, and A. H. Sobel, 2009: Delayed Sahel rainfall and global seasonal cycle in a warmer climate. *Geophys. Res. Lett.*, **36**, L23707, https://doi.org/10.1029/2009GL041303.

——, ——, and S. J. Camargo, 2009: The role of the Sahara low in summertime Sahel rainfall variability and change in the CMIP3 models. *J. Climate*, **22**, 5755–5771, https://doi.org/10.1175/2009JCLI2969.1.

Birner, T., S. M. Davis, and D. J. Seidel, 2014: The changing width of Earth's tropical belt. *Phys. Today*, **67**, 38, https://doi.org/10.1063/PT.3.2620.

Black, E., J. Slingo, and K. R. Sperber, 2003: An observational study of the relationship between excessively strong short rains in coastal East Africa and Indian Ocean SST. *Mon. Wea. Rev.*, **131**, 74–94, https://doi.org/10.1175/1520-0493(2003)131<0074:AOSOTR>2.0.CO;2.

——, H. Greatrex, M. Young, and R. Maidment, 2016: Incorporating satellite data into weather index insurance. *Bull. Amer. Meteor. Soc.*, **97**, ES203–ES206, https://doi.org/10.1175/BAMS-D-16-0148.1.

Boyard-Micheau, J., P. Camberlin, N. Philippon, and V. Moron, 2013: Regional-scale rainy season onset detection: A new approach based on multivariate analysis. *J. Climate*, **26**, 8916–8928, https://doi.org/10.1175/JCLI-D-12-00730.1.

Camberlin, P., V. Moron, R. Okoola, N. Philippon, and W. Gitau, 2009: Components of rainy seasons variability in equatorial East Africa: Onset, cessation, rainfall frequency and intensity. *Theor. Appl. Climatol.*, **98**, 237–249, https://doi.org/10.1007/s00704-009-0113-1.

Chauvin, F., R. Roehrig, and J.-P. Lafore, 2010: Intraseasonal variability of the Saharan heat low and its link with midlatitudes. *J. Climate*, **23**, 2544–2561, https://doi.org/10.1175/2010JCLI3093.1.

Chou, C., J. C. Chiang, C.-W. Lan, C.-H. Chung, Y.-C. Liao, and C.- J. Lee, 2013: Increase in the range between wet and dry season precipitation. *Nat. Geosci.*, **6**, 263–267, https://doi.org/10.1038/ngeo1744.

Christensen, J. H., K. K. Kanikicharla, G. Marshall, and J. Turner, 2013: Climate phenomena and their relevance for future regional climate change. *Climate Change 2013: The Physical Science Basis*, T. F. Stocker et al., Eds., Cambridge University Press, 1217–1308.

Collins, M., and Coauthors, 2013: Long-term climate change: Projections, commitments and irreversibility. *Climate Change 2013: The Physical Science Basis*, T. F. Stocker et al., Eds., Cambridge University Press, 1029–1136.

Cook, C., C. J. Reason, and B. C. Hewitson, 2004: Wet and dry spells within particularly wet and dry summers in the South African summer rainfall region. *Climate Res.*, **26**, 17–31, https://doi.org/10.3354/cr026017.

Cook, K. H., and E. K. Vizy, 2012: Impact of climate change on mid-twenty-first century growing seasons in Africa. *Climate Dyn.*, **39**, 2937–2955, https://doi.org/10.1007/s00382-012-1324-1.

Crétat, J., B. Pohl, B. Dieppois, S. Berthou, and J. Pergaud, 2018: The Angola low: Relationship with southern African rainfall and ENSO. *Climate Dyn.*, https://doi.org/10.1007/s00382-018-4222-3, in press.

Cubasch, U., and Coauthors, 2001: Projections of future climate change. *Climate Change 2001: The Scientific Basis*, J. T. Houghton et al., Eds. Cambridge University Press, 525–582.

Diaconescu, E. P., P. Gachon, J. Scinocca, and R. Laprise, 2015: Evaluation of daily precipitation statistics and monsoon onset/retreat over western Sahel in multiple data sets. *Climate Dyn.*, **45**, 1325–1354, https://doi.org/10.1007/s00382-014-2383-2.

Dixon, R. D., A. S. Daloz, D. J. Vimont, and M. Biasutti, 2017: Saharan heat low biases in CMIP5 models. *J. Climate*, **30**, 2867–2884, https://doi.org/10.1175/JCLI-D-16-0134.1.

——, D. J. Vimont, and A. S. Daloz, 2018: The relationship between tropical precipitation biases and the Saharan heat low bias in CMIP5 models. *Climate Dyn.*, **50**, 3729–3744, https://doi.org/10.1007/s00382-017-3838-z.

Dong, B., and R. Sutton, 2015: Dominant role of greenhouse-gas forcing in the recovery of Sahel rainfall. *Nat. Climate Change*, **5**, 757–760, https://doi.org/10.1038/nclimate2664.

d'Orgeval, T., J. Polcher, and L. Li, 2006: Uncertainties in modelling future hydrological change over West Africa. *Climate Dyn.*, **26**, 93–108, https://doi.org/10.1007/s00382-005-0079-3.

Dunning, C. M., E. C. Black, and R. P. Allan, 2016: The onset and cessation of seasonal rainfall over Africa. *J. Geophys. Res. Atmos.*, **121**, 11 405–11 424, https://doi.org/10.1002/2016JD025428.

——, R. P. Allan, and E. Black, 2017: Identification of deficiencies in seasonal rainfall simulated by CMIP5 climate models. *Environ. Res. Lett.*, **12**, 114001, https://doi.org/10.1088/1748-9326/aa869e.

Dwyer, J. G., M. Biasutti, and A. H. Sobel, 2014: The effect of greenhouse gas–induced changes in SST on the annual cycle of zonal mean tropical precipitation. *J. Climate*, **27**, 4544–4565, https://doi.org/10.1175/JCLI-D-13-00216.1.

Evan, A. T., C. Flamant, C. Lavaysse, C. Kocha, and A. Saci, 2015: Water vapor–forced greenhouse warming over the Sahara Desert and the recent recovery from the Sahelian drought. *J. Climate*, **28**, 108–123, https://doi.org/10.1175/JCLI-D-14-00039.1.

Feng, X., A. Porporato, and I. Rodriguez-Iturbe, 2013: Changes in rainfall seasonality in the tropics. *Nat. Climate Change*, **3**, 811–815, https://doi.org/10.1038/nclimate1907.

Frank, E., H. Eakin, and D. López-Carr, 2011: Social identity, perception and motivation in adaptation to climate risk in the coffee sector of Chiapas, Mexico. *Global Environ. Change*, **21**, 66–76, https://doi.org/10.1016/j.gloenvcha.2010.11.001.

Funk, C., M. D. Dettinger, J. C. Michaelsen, J. P. Verdin, M. E. Brown, M. Barlow, and A. Hoell, 2008: Warming of the Indian Ocean threatens eastern and southern African food security but could be mitigated by agricultural development. *Proc. Natl. Acad. Sci. USA*, **105**, 11 081–11 086, https://doi.org/10.1073/pnas.0708196105.

——, and Coauthors, 2015: The Climate Hazards Infrared Precipitation with Stations—A new environmental record for monitoring extremes. *Sci. Data*, **2**, 150066, https://doi.org/10.1038/sdata.2015.66.

Held, I. M., and B. J. Soden, 2006: Robust responses of the hydrological cycle to global warming. *J. Climate*, **19**, 5686–5699, https://doi.org/10.1175/JCLI3990.1.

Howard, E., and R. Washington, 2018: Characterizing the synoptic expression of the Angola low. *J. Climate*, **31**, 7147–7165, https://doi.org/10.1175/JCLI-D-18-0017.1.

Huffman, G. J., R. F. Adler, M. M. Morrissey, D. T. Bolvin, S. Curtis, R. Joyce, B. McGavock, and J. Susskind, 2001: Global precipitation at one-degree daily resolution from multisatellite observations. *J. Hydrometeor.*, **2**, 36–50, https://doi.org/10.1175/1525-7541(2001)002<0036:GPAODD>2.0.CO;2.

Hulme, M., R. Doherty, T. Ngara, M. New, and D. Lister, 2001: African climate change: 1900–2100. *Climate Res.*, **17**, 145–168, https://doi.org/10.3354/cr017145.

Hutchins, A., A. Tamargo, C. Bailey, and Y. Kim, 2015: Assessment of climate change impacts on cocoa production and approaches to adaptation and mitigation: A contextual view of Ghana and Costa Rica. 22 pp., https://elliott.gwu.edu/sites/g/files/zaxdzs2141/f/World%20Cocoa%20Foundation.pdf.

Issa Lélé, M., and P. J. Lamb, 2010: Variability of the intertropical front (ITF) and rainfall over the West African Sudan–Sahel zone. *J. Climate*, **23**, 3984–4004, https://doi.org/10.1175/2010JCLI3277.1.

Joshi, M. M., J. M. Gregory, M. J. Webb, D. M. Sexton, and T. C. Johns, 2008: Mechanisms for the land/sea warming contrast exhibited by simulations of climate change. *Climate Dyn.*, **30**, 455–465, https://doi.org/10.1007/s00382-007-0306-1.

Kniveton, D. R., R. Layberry, C. J. R. Williams, and M. Peck, 2009: Trends in the start of the wet season over Africa. *Int. J. Climatol.*, **29**, 1216–1225, https://doi.org/10.1002/joc.1792.

Konare, A., A. Zakey, F. Solmon, F. Giorgi, S. Rauscher, S. Ibrah, and X. Bi, 2008: A regional climate modeling study of the effect of desert dust on the West African monsoon. *J. Geophys. Res.*, **113**, D12206, https://doi.org/10.1029/2007JD009322.

Lambert, F. H., M. J. Webb, and M. M. Joshi, 2011: The relationship between land–ocean surface temperature contrast and radiative forcing. *J. Climate*, **24**, 3239–3256, https://doi.org/10.1175/2011JCLI3893.1.

Lavaysse, C., C. Flamant, S. Janicot, D. Parker, J.-P. Lafore, B. Sultan, and J. Pelon, 2009: Seasonal evolution of the West African heat low: A climatological perspective. *Climate Dyn.*, **33**, 313–330, https://doi.org/10.1007/s00382-009-0553-4.

Lazenby, M. J., M. C. Todd, and Y. Wang, 2016: Climate model simulation of the South Indian Ocean convergence zone: Mean state and variability. *Climate Res.*, **68**, 59–71, https://doi.org/10.3354/cr01382.

——, ——, R. Chadwick, and Y. Wang, 2018: Future precipitation projections over central and southern Africa and the adjacent Indian Ocean: What causes the changes and the uncertainty? *J. Climate*, **31**, 4807–4826, https://doi.org/10.1175/JCLI-D-17-0311.1.

Lee, J.-Y., and B. Wang, 2014: Future change of global monsoon in the CMIP5. *Climate Dyn.*, **42**, 101–119, https://doi.org/10.1007/s00382-012-1564-0.

Liebmann, B., I. Bladé, G. N. Kiladis, L. M. Carvalho, G. B. Senay, D. Allured, S. Leroux, and C. Funk, 2012: Seasonality of African precipitation from 1996 to 2009. *J. Climate*, **25**, 4304–4322, https://doi.org/10.1175/JCLI-D-11-00157.1.

——, and Coauthors, 2017: Climatology and interannual variability of boreal spring wet season precipitation in the eastern Horn of Africa and implications for its recent decline. *J. Climate*, **30**, 3867–3886, https://doi.org/10.1175/JCLI-D-16-0452.1.

Maidment, R. I., D. Grimes, R. P. Allan, E. Tarnavsky, M. Stringer, T. Hewison, R. Roebeling, and E. Black, 2014: The 30 year TAMSAT African Rainfall Climatology and Time Series (TARCAT) data set. *J. Geophys. Res. Atmos.*, **119**, 10 619–10 644, https://doi.org/10.1002/2014JD021927.

——, R. P. Allan, and E. Black, 2015: Recent observed and simulated changes in precipitation over Africa. *Geophys. Res. Lett.*, **42**, 8155–8164, https://doi.org/10.1002/2015GL065765.

——, and Coauthors, 2017: A new, long-term daily satellite-based rainfall dataset for operational monitoring in Africa. *Sci. Data*, **4**, 170063, https://doi.org/10.1038/sdata.2017.63.

Marteau, R., V. Moron, and N. Philippon, 2009: Spatial coherence of monsoon onset over western and central Sahel (1950–2000). *J. Climate*, **22**, 1313–1324, https://doi.org/10.1175/2008JCLI2383.1.

Marvel, K., M. Biasutti, C. Bonfils, K. E. Taylor, Y. Kushnir, and B. I. Cook, 2017: Observed and projected changes to the precipitation annual cycle. *J. Climate*, **30**, 4983–4995, https://doi.org/10.1175/JCLI-D-16-0572.1.

Monerie, P.-A., P. Roucou, and B. Fontaine, 2013: Mid-century effects of climate change on African monsoon dynamics using the A1B emission scenario. *Int. J. Climatol.*, **33**, 881–896, https://doi.org/10.1002/joc.3476.

——, M. Biasutti, and P. Roucou, 2016: On the projected increase of Sahel rainfall during the late rainy season. *Int. J. Climatol.*, **36**, 4373–4383, https://doi.org/10.1002/joc.4638.

——, E. Sanchez-Gomez, and J. Boé, 2017: On the range of future Sahel precipitation projections and the selection of a subsample of CMIP5 models for impact studies. *Climate Dyn.*, **48**, 2751–2770, https://doi.org/10.1007/s00382-016-3236-y.

Munday, C., and R. Washington, 2017: Circulation controls on southern African precipitation in coupled models: The role of the Angola low. *J. Geophys. Res. Atmos.*, **122**, 861–877, https://doi.org/10.1002/2016JD025736.

Nicholson, S. E., 2000: The nature of rainfall variability over Africa on time scales of decades to millennia. *Global Planet. Change*, **26**, 137–158, https://doi.org/10.1016/S0921-8181(00)00040-0.

——, 2013: The West African Sahel: A review of recent studies on the rainfall regime and its interannual variability. *ISRN Meteor.*, **2013**, 453521, https://doi.org/10.1155/2013/453521.

——, 2017: Climate and climatic variability of rainfall over eastern Africa. *Rev. Geophys.*, **55**, 590–635, https://doi.org/10.1002/2016RG000544.

Park, J.-Y., J. Bader, and D. Matei, 2016: Anthropogenic Mediterranean warming essential driver for present and future Sahel rainfall. *Nat. Climate Change*, **6**, 941–945, https://doi.org/10.1038/nclimate3065.

Parker, D., and M. Diop-Kane, Eds., 2017: *Meteorology of Tropical West Africa: The Forecaster's Handbook*. Wiley-Blackwell, 496 pp.

Pohl, B., C. Macron, and P.-A. Monerie, 2017: Fewer rainy days and more extreme rainfall by the end of the century in southern Africa. *Sci. Rep.*, **7**, 46466, https://doi.org/10.1038/srep46466.

Reason, C., W. Landman, and W. Tennant, 2006: Seasonal to decadal prediction of southern African climate and its links with variability of the Atlantic Ocean. *Bull. Amer. Meteor. Soc.*, **87**, 941–955, https://doi.org/10.1175/BAMS-87-7-941.

Riahi, K., and Coauthors, 2011: RCP8.5—A scenario of comparatively high greenhouse gas emissions. *Climatic Change*, **109**, 33–57, https://doi.org/10.1007/s10584-011-0149-y.

Rosenthal, E., 2011: Heat damages Colombia coffee, raising prices. *The New York Times*, 9 March 2011, https://www.nytimes.com/2011/03/10/science/earth/10coffee.html.

Rowell, D. P., C. A. Senior, M. Vellinga, and R. J. Graham, 2016: Can climate projection uncertainty be constrained over Africa using metrics of contemporary performance? *Climatic Change*, **134**, 621–633, https://doi.org/10.1007/s10584-015-1554-4.

Schmetz, J., P. Pili, S. Tjemkes, D. Just, J. Kerkmann, S. Rota, and A. Ratier, 2002: An introduction to Meteosat second generation (MSG). *Bull. Amer. Meteor. Soc.*, **83**, 977–992, https://doi.org/10.1175/1520-0477(2002)083<0977:AITMSG>2.3.CO;2.

Seidel, D. J., Q. Fu, W. J. Randel, and T. J. Reichler, 2008: Widening of the tropical belt in a changing climate. *Nat. Geosci.*, **1**, 21–24, https://doi.org/10.1038/ngeo.2007.38.

Seth, A., S. A. Rauscher, M. Biasutti, A. Giannini, S. J. Camargo, and M. Rojas, 2013: CMIP5 projected changes in the annual cycle of precipitation in monsoon regions. *J. Climate*, **26**, 7328–7351, https://doi.org/10.1175/JCLI-D-12-00726.1.

Shongwe, M. E., G. J. van Oldenborgh, B. van den Hurk, B. de Boer, C. Coelho, and M. van Aalst, 2009: Projected changes in mean and extreme precipitation in Africa under global warming. Part I: Southern Africa. *J. Climate*, **22**, 3819–3837, https://doi.org/10.1175/2009JCLI2317.1.

——, ——, ——, and M. van Aalst, 2011: Projected changes in mean and extreme precipitation in Africa under global warming. Part II: East Africa. *J. Climate*, **24**, 3718–3733, https://doi.org/10.1175/2010JCLI2883.1.

Shonk, J. K., E. Guilyardi, T. Toniazzo, S. J. Woolnough, and T. Stockdale, 2018: Identifying causes of western Pacific ITCZ drift in ECMWF System 4 hindcasts. *Climate Dyn.*, **50**, 939–954, https://doi.org/10.1007/s00382-017-3650-9.

Sillmann, J., V. Kharin, F. Zwiers, X. Zhang, and D. Bronaugh, 2013: Climate extremes indices in the CMIP5 multimodel ensemble: Part 2. Future climate projections. *J. Geophys. Res. Atmos.*, **118**, 2473–2493, https://doi.org/10.1002/jgrd.50188.

Solmon, F., M. Mallet, N. Elguindi, F. Giorgi, A. Zakey, and A. Konaré, 2008: Dust aerosol impact on regional precipitation over western Africa, mechanisms and sensitivity to absorption properties. *Geophys. Res. Lett.*, **35**, L24705, https://doi.org/10.1029/2008GL035900.

Sultan, B., and S. Janicot, 2003: The West African monsoon dynamics. Part II: The "preonset" and "onset" of the summer monsoon. *J. Climate*, **16**, 3407–3427, https://doi.org/10.1175/1520-0442(2003)016<3407:TWAMDP>2.0.CO;2.

Sutton, R. T., B. Dong, and J. M. Gregory, 2007: Land/sea warming ratio in response to climate change: IPCC AR4 model results and comparison with observations. *Geophys. Res. Lett.*, **34**, L02701, https://doi.org/10.1029/2006GL028164.

Sylla, M. B., F. Giorgi, J. S. Pal, P. Gibba, I. Kebe, and M. Nikiema, 2015: Projected changes in the annual cycle of high-intensity

precipitation events over West Africa for the late twenty-first century. *J. Climate*, **28**, 6475–6488, https://doi.org/10.1175/JCLI-D-14-00854.1.

Tanser, F. C., B. Sharp, and D. Le Sueur, 2003: Potential effect of climate change on malaria transmission in Africa. *Lancet*, **362**, 1792–1798, https://doi.org/10.1016/S0140-6736(03)14898-2.

Tarnavsky, E., D. Grimes, R. Maidment, E. Black, R. P. Allan, M. Stringer, R. Chadwick, and F. Kayitakire, 2014: Extension of the TAMSAT satellite-based rainfall monitoring over Africa and from 1983 to present. *J. Appl. Meteor. Climatol.*, **53**, 2805–2822, https://doi.org/10.1175/JAMC-D-14-0016.1.

Taylor, C. M., and Coauthors, 2017: Frequency of extreme Sahelian storms tripled since 1982 in satellite observations. *Nature*, **544**, 475–478, https://doi.org/10.1038/nature22069.

Taylor, K. E., R. J. Stouffer, and G. A. Meehl, 2012: An overview of CMIP5 and the experiment design. *Bull. Amer. Meteor. Soc.*, **93**, 485–498, https://doi.org/10.1175/BAMS-D-11-00094.1.

Thomson, A. M., and Coauthors, 2011: RCP4.5: A pathway for stabilization of radiative forcing by 2100. *Climatic Change*, **109**, 77–94, https://doi.org/10.1007/s10584-011-0151-4.

Tierney, J. E., C. C. Ummenhofer, and P. B. deMenocal, 2015: Past and future rainfall in the Horn of Africa. *Sci. Adv.*, **1**, e1500682, https://doi.org/10.1126/sciadv.1500682.

van Vuuren, D. P., and Coauthors, 2011: The representative concentration pathways: An overview. *Climatic Change*, **109**, 5–31, https://doi.org/10.1007/s10584-011-0148-z.

Vizy, E. K., and K. H. Cook, 2017: Seasonality of the observed amplified Sahara warming trend and implications for Sahel rainfall. *J. Climate*, **30**, 3073–3094, https://doi.org/10.1175/JCLI-D-16-0687.1.

——, ——, J. Chimphamba, and B. McCusker, 2015: Projected changes in Malawi's growing season. *Climate Dyn.*, **45**, 1673–1698, https://doi.org/10.1007/s00382-014-2424-x.

Yang, W., R. Seager, M. A. Cane, and B. Lyon, 2015a: The annual cycle of East African precipitation. *J. Climate*, **28**, 2385–2404, https://doi.org/10.1175/JCLI-D-14-00484.1.

——, ——, ——, and ——, 2015b: The rainfall annual cycle bias over East Africa in CMIP5 coupled climate models. *J. Climate*, **28**, 9789–9802, https://doi.org/10.1175/JCLI-D-15-0323.1.

Zhang, L., P. Wu, T. Zhou, M. J. Roberts, and R. Schiemann, 2016: Added value of high resolution models in simulating global precipitation characteristics. *Atmos. Sci. Lett.*, **17**, 646–657, https://doi.org/10.1002/asl.715.

Zheng, X.-T., S.-P. Xie, Y. Du, L. Liu, G. Huang, and Q. Liu, 2013: Indian Ocean dipole response to global warming in the CMIP5 multimodel ensemble. *J. Climate*, **26**, 6067–6080, https://doi.org/10.1175/JCLI-D-12-00638.1.